Spatial distributions of atomic hydrogen and C2 in an oxyacetylene flame in relation to diamond growth

Spatial distributions of atomic hydrogen and C_2 in an oxyacetylene flame in relation to diamond growth

R. J. H. Klein-Douwel[a] and J. J. ter Meulen
Department of Molecular and Laser Physics, University of Nijmegen, Toernooiveld, 6525 ED Nijmegen, The Netherlands

(Received 13 June 1997; accepted for publication 18 January 1998)

Two-dimensional laser induced fluorescence measurements are applied to the chemical vapour deposition of diamond by an oxyacetylene flame to visualize the distributions of atomic hydrogen and C_2 in the gas phase during diamond growth. Experiments are carried out in both laminar and turbulent flames and reveal that atomic hydrogen is ubiquitous at and beyond the flame front. Its presence extends to well outside the diamond deposition region, whereas the C_2 distribution is limited to the flame front and the acetylene feather. The diamond layers obtained are characterized by optical as well as scanning electron microscopy and Raman spectroscopy. Clear relations are observed between the local variations in growth rate and quality of the diamond layer and the distribution of H and C_2 in the boundary layer just above the substrate. These relations agree with theoretical models describing their importance in (flame) deposition processes of diamond. Three separate regions can be discerned in the flame and the diamond layer, where the gas phase and diamond growth are predominantly governed by the flame source gases, the ambient atmosphere, and the interaction of both, respectively. © *1998 American Institute of Physics.* [S0021-8979(98)08008-6]

I. INTRODUCTION

Diamond is an attractive and promising material for a variety of applications, including many industrial ones, due to its excellent properties like hardness, wear resistance, chemical inertia, high index of refraction and optical transparency over a large range of the spectrum, to name but a few.[1,2] In 1988 Hirose and Kondo[3] reported diamond growth in a laminar oxyacetylene flame, operated with a small excess of acetylene. Flame deposition of diamond has since been well established and many gas phase diagnostic techniques have been applied to determine the growth mechanism of diamond (see Ref. 4 and references therein).

Many hypotheses have been proposed for the role of hydrogen atoms in chemical vapor deposition (CVD) diamond film growth. It is generally believed that hydrogen atoms incident on the surface abstract hydrogen to produce vacant sites, where growth species can then stick to the diamond layer,[5] and that atomic hydrogen etches surface graphite.[6] Gas phase hydrogen atoms may also produce condensable carbon radicals by reactions with hydrocarbons,[7] and, impinging on the surface, they may create surface radicals[8–10] and refill vacant sites by adsorption.[8,11] Once adsorbed, atomic hydrogen may also stabilize the diamond surface structure.[12–14] The role of atomic hydrogen in diamond CVD has been studied from a theoretical point of view by several authors, including Frenklach *et al.*,[15–17] Matsui *et al.*,[18,19] Janssen *et al.*,[12] Harris,[20,21] and Goodwin.[22–24] Okkerse *et al.* have recently presented a compact gas phase and surface reaction mechanism that can be used in multidimensional simulations of diamond growth in oxyacetylene flames.[25] Experimental investigations on the surface role of H have been carried out by Ohl *et al.*[26] and Butler and co-workers,[27] among others. Studies on atomic hydrogen in the gas phase of CVD systems have been carried out in a hot filament reactor by resonance enhanced multi-photon ionization[28] and two-photon laser induced fluorescence (LIF),[29,30] which technique has also been used in a rf plasma reactor[31,32] and a microwave reactor.[33]

In the present work the two-dimensional laser induced fluorescence (2D-LIF) technique is applied to measure the distributions of atomic hydrogen and C_2 in the oxyacetylene flame during diamond growth. LIF is a powerful method to diagnosticize gaseous combustion processes *in situ*, due to its species specificity, high sensitivity and non-intrusiveness. If pulsed lasers and charge coupled device (CCD) cameras are applied, non-stationary processes, such as turbulent flames, can be studied as well.

Since the first excited state of atomic hydrogen lies 10.2 eV above the ground state, multi-photon excitation has to be used. Goldsmith[34,35] and Dowling *et al.*[31] have compared several excitation and detection schemes for LIF of atomic hydrogen. Goldsmith and Anderson have excited H by $2\times243+656$ nm and observed 656 nm fluorescence[36] to obtain a 2D atomic hydrogen distribution in a laminar hydrogen-air diffusion flame. This technique cannot be used in the present experimental setup, because reflections of the laser beam off the substrate would saturate the CCD camera. Hence excitation to the $n=3$ level at 2×205 nm and detection of the $n=3 \rightarrow n=2$ transition at 656 nm is employed in the present work. Photochemical effects of the 205 nm light on the flame gases[31,35,37] and stimulated emission due to the population inversion in the $n=1$, 2, and 3 levels of atomic hydrogen[38,39] are avoided by decreasing the laser power den-

[a]Electronic mail: robertkd@sci.kun.nl

sity. In low pressure environments the collisional quenching of the fluorescence signal can be determined[37,40] and the H LIF signal can be quantified by comparison to measurements in a calibration reactor where the H concentration is known.[29,31,32] At atmospheric pressure, however, quantification of the signal is hampered by collisional quenching of the fluorescence, which not only depends on temperature and pressure, but also on the nature of the collision partners. Since at atmospheric pressure many collisions will take place during the fluorescence lifetime and a multitude of different species is available to collide with, quantitative measurements are not attempted and the results therefore will be interpreted in a more qualitative way.

In contrast to the large amount of theoretical and experimental work on atomic hydrogen in diamond CVD systems, fewer studies have been reported on the role of C_2. Two-dimensional imaging of C_2 by LIF in hydrocarbon-air flames has already been performed in 1986 by Allen and co-workers,[41] but was first applied to a diamond depositing oxyacetylene flame by Klein-Douwel *et al.*[4] Kaminski and Ewart[42] performed absolute C_2 concentration measurements by LIF in a low-pressure microwave reactor growing diamond from H_2, Ar, and CH_4. Theoretical as well as experimental work on the role of C_2 as a possible growth species for diamond has been carried out by Gruen and co-workers. They have grown diamond from an Ar/C_{60} plasma and ascribe their relatively high growth rates to the direct incorporation of C_2 into the diamond lattice.[43,44] Experiments in a hydrogen/argon/methane plasma in the same group have also shown a positive relation between C_2 and the diamond growth rate. Calculations show that insertion of C_2 into a (100) diamond surface is energetically favourable.[45] Further calculations show that C_2 addition to a (110) surface is exothermic as well.[46,47] Additional references on optical diagnostics of C_2 in diamond growth processes are given in the previous work on C_2.[4]

II. EXPERIMENTAL SETUP

A. Diamond growth and characterization

The deposition setup is described in detail in previous work[4,48] and is almost identical to the one used by Schermer and co-workers.[49–51] A polycrystalline diamond layer is deposited onto a water cooled molybdenum substrate by a commercially available welding torch (orifice diameter 1.4 mm), burning acetylene and oxygen (both from Indugas). Most experiments concerned in this work are performed with laminar burners, but in a few a turbulent burner of Centre Suisse d'Electronique et de Microtechnique (CSEM) design is used,[52] which has the same exit opening but a turbulence inducing step inside[53] and has been used by Schermer and co-workers as well.[50,51,53] All burners are operated with a total gas flow of $\approx$6 standard liters per minute (SLM).

There are three main experimental parameters in the diamond deposition process in an oxyacetylene flame: the distance d between the substrate and the tip of the flame front, the deposition temperature T_d at the growing diamond surface, and the acetylene supersaturation S_{ac}. The temperature T_d is kept constant at 1050 ± 20 °C by means of a pulsed water vaporizer, which is controlled by a thermocouple located about 2.5 mm beneath the center of the substrate surface. Both the oxygen and acetylene flow are regulated by mass flow controllers, but while the oxygen flow f_{ox} is fixed at 3.0 SLM, the acetylene flow is determined by the desired value of S_{ac}. The supersaturation S_{ac} is defined as the percentage of additional acetylene flow compared to the acetylene flow of the neutral flame, which is neither fuel rich nor oxygen rich and shows a distinct, conical flame front in a laminar flame. Unless explicitly stated otherwise, $S_{ac}=5\%$ and the aforementioned values of T_d, f_{ox} and burner orifice diameter are used in all experiments. The typical deposition time in the experiments is between 1 and 2 h.

From previous studies it is known that a value for d between 1 and 2 mm, $T_d\approx1050$ °C and $S_{ac}\approx5\%$ yield optimum diamond growth conditions.[4,48–51,53] These studies also show, however, that the diamond layer characteristics and the species distributions in the gas phase are significantly affected by the distance between substrate and flame front. In order to study these effects in more detail, d is varied in this work between 0.3 and 4.1 mm, where the precise value of d is determined with a CCD camera.[4] In one experiment on C_2, performed at $d=1.52$ mm, a different laminar burner (orifice diameter 1.6 mm) and $T_d=1150$ °C and $f_{ox}=2.84$ SLM are used for the purpose of comparison to previous work on C_2.[4]

The experiments are carried out in ambient air, with the flame burning at atmospheric pressure. After growth the diamond layers are characterized by optical differential interference contrast microscopy (DICM), scanning electron microscopy (SEM) and Raman spectroscopy. The optical microscope is also used to determine the thickness of the diamond layer along the path of the laser beam, which together with the total deposition time yields the deposition rate v_d with an accuracy of ±5 μm/h. The exact procedure has been described previously.[49] Raman spectra are taken along the path of the laser sheet at radially different positions of the diamond layer by focusing a 514 nm Ar^+ laser beam to a spot size of ≈30 μm. In order to quantify the quality of the layer a quality factor Q is used: it is defined as 1000 times the area of the diamond peak in the Raman spectrum divided by the area of the background between 1100 and 1700 cm^{-1}.[49] High Q values ($Q\gtrsim10$ for flame deposited polycrystalline diamond layers) correspond to high purity diamond, whereas low Q values ($Q\lesssim10$) indicate a high non-diamond carbon content and/or a high fluorescence background of the deposited layer.

B. Two-photon LIF of atomic hydrogen

The laser system consists of a Nd: yttrium–aluminum–garnet (YAG) pumped tunable dye laser (Quantel YG 781 + TDL 50), operating on Sulforhodamine 640. The system delivers 5 ns laser pulses with a repetition frequency of 10 Hz and an output pulse energy of 55 mJ at 615 nm. The 205 nm UV laser radiation is generated by frequency doubling the 615 nm in a potassium dihydrogen phosphate (KDP) crystal and subsequent frequency mixing of the resulting 307.5 nm with the residual 615 nm in a beta-barium borate (BBO)

crystal. The polarization of the 307.5 nm light is 90° rotated with respect to that of the 615 nm light, but for frequency mixing both polarizations have to be parallel. Therefore a $\lambda/2$ plate for 615 nm located between the KDP and BBO crystals is used to rotate the polarization of the red laser light. The resulting 205 nm laser radiation has a bandwidth of ≈ 0.2 cm^{-1} and is separated from the other two wavelengths by means of a Pellin-Broca prism. The typical pulse energy at the position of the flame is 0.4 mJ.

The laser beam is transformed into a sheet using two cylindrical lenses ($f=28$ and $f=4.5$ cm) acting as a telescope in horizontal direction, and a third cylindrical lens ($f=41$ cm) making the beam slightly divergent in vertical direction. The resulting laser sheet is directed through the center of the flame where it is 4 mm high and 0.3 mm thin, yielding a typical power density of 6.7 MW/cm^2. Fluorescence images recorded in this way therefore represent a cross section of the flame. During diamond growth experiments the lower edge of the laser sheet is directed below the substrate surface and is therefore cut off, thus ensuring enough laser intensity just above the substrate.

Atomic hydrogen fluorescence is detected at right angles to the laser beam by a Peltier cooled CCD camera, equipped with an image intensifier (La Vision FlameStar II, 384×286 pixels, 12 bits dynamical range). The very strong natural emission of the flame itself is suppressed by a factor of 5×10^6 by switching on the image intensifier for only 20 ns at every trigger pulse. The CCD signal is sent to a personal computer, where it is digitized and further processed. Two-dimensional images of the flame and atomic hydrogen fluorescence are collected by the camera system with a UV-Nikkor 105 mm f/4.5 objective combined with expandable bellows in front of it, giving a spatial resolution of 35 μm per pixel. The experimental spatial accuracy of the camera system is estimated to be 2 to 3 pixels, or about 80 μm in this case. Use of the Micro-Nikkor 200 mm f/4.0 objective, which is not transparent in the UV, would yield a higher spatial resolution, but because Rayleigh scattering of the laser sheet also has to be recorded (as discussed below), this is not an option. The scattered laser radiation from the substrate and the natural emission of the flame are suppressed by a 656 nm transmission interference filter [10 nm full width at half maximum (FWHM)].

Because the atomic hydrogen is excited by a two-photon transition, the fluorescence signal should vary with the square of the laser power. If the power dependence of the fluorescence signal is less than quadratic, ionization of the excited hydrogen may be important, decreasing the fluorescence yield. On the other hand, if the power dependence is higher than quadratic, laser induced photochemical processes may be taking place in which atomic hydrogen is created from flame species by one or more 205 nm photon(s) and excited by two subsequent 205 nm photons in the same laser pulse. In order to check this, the power dependence is measured in the freely burning flame, i.e., when no substrate is present. The $f=41$ cm cylindrical lens is temporarily removed for this measurement, decreasing the size of the laser beam, to increase the available laser power density. Variation of the 205 nm laser power is in this case achieved by slightly rotating the $\lambda/2$ plate, which influences the frequency mixing efficiency in the BBO crystal.

Once the quadratic power dependence of the fluorescence signal has been established, images of the atomic hydrogen fluorescence distribution can be measured in the flame during diamond growth. Although this is in principle possible using a single laser shot, 50 to 140 laser shots (depending on the actual laser power) are integrated on the CCD chip in order to reach its full dynamical range. The H fluorescence image is then obtained by recording an image with the laser tuned exactly to the two-photon transition frequency, immediately afterwards recording an image with the laser tuned off resonance, and subtracting the two images.

Since the vertical intensity distribution in the laser sheet is not homogeneous enough, it is determined after every experiment by recording the two-dimensional Rayleigh scattering of the 205 nm laser sheet in ambient air. In order to image the Rayleigh scattered signal, the burner and the substrate are moved out of the camera's field of view, and the 656 nm interference filter (normally in front of the UV-Nikkor objective) is removed as well, leaving the laser sheet and the detection geometry intact. The difference between the on and off resonance images is divided by the square of the Rayleigh scattering image, yielding the laser power normalized atomic hydrogen fluorescence distribution. Absorption of the 205 nm laser light by the flame is measured by a Scientech power meter, located behind the flame, to be $\approx 15\%$. There will be local differences, however, in the UV absorption, for the absorbing species column density will vary in the flame as a function of height above the substrate. It turns out that absorption can be neglected in the region of interest (less than 0.5 mm above the substrate), hence the H LIF images are not corrected for laser beam absorption.

Natural emission of the flame, if observed through the 656 nm interference filter, only consists of chemiluminescence of C_2: (a part of) the $v'=2\rightarrow v''=5$, $3\rightarrow 6$, and $4\rightarrow 7$ bands of the C_2 Swan system as emitted by the flame[54] is transmitted by the filter. Emission images obtained through the interference filter give the distribution of excited C_2 in the flame and yield the dimensions of the flame front and the acetylene feather.

C. LIF of C_2

LIF measurements of the distribution of C_2 in laminar oxyacetylene flames during diamond deposition have already been described in a previous study,[4] but in that work d was limited between 0.58 and 1.41 mm. In this work d is varied beyond that range and turbulent flames are examined as well. C_2 is detected by exciting the $d^3\Pi_g(v'=2)\leftarrow a^3\Pi_u(v''=0)$ transition around 438 nm (Swan system). The dye laser is operated with Coumarine 440, resulting in typically 0.8 mJ/pulse at 438 nm (bandwidth 0.15 cm^{-1}) at the location of the burner. The UV-Nikkor objective is replaced by the Micro-Nikkor 200 mm f/4.0 objective to obtain a spatial resolution of 20 μm per pixel and a long-pass filter transmitting only $\lambda \geqslant 470$ nm is used in front of it, which allows the detection of the $d^3\Pi_g(v')\rightarrow a^3\Pi_u(v'')$, $v'-v''\leqslant 1$ fluorescence for

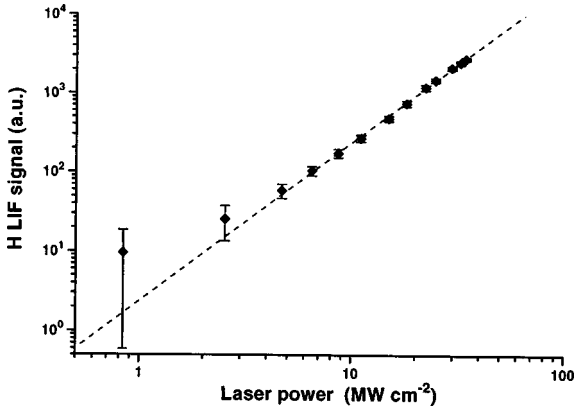

FIG. 1. Atomic hydrogen LIF signal at 656 nm after two-photon excitation vs the laser power at 205 nm (the size of the laser sheet is constant). The dashed line is a quadratic fit (slope: 2) to the data points. Due to the logarithmic scale, the deviation from the quadratic fit of the two lowest lying data points appears to be more significant than it is.

v' up to 4.[54] Fluorescence from the $v' \neq 2$ levels is due to collisional redistribution of population in the $d^3\Pi_g$ state.

In the laminar flame measurements two laser shots are integrated on the CCD chip to increase the signal-to-noise ratio. In the turbulent flame 100 laser shots are integrated to obtain an averaged image which does not change in time anymore. The gain of the CCD image intensifier is correspondingly lower in this case.

At the laser powers used for imaging C_2, the fluorescence signal is still linear with the laser intensity, which allows correction for the inhomogeneity of the vertical intensity profile of the laser beam. Rayleigh scattering is used in the case of atomic hydrogen to correct for this, but since the Rayleigh scattering signal intensity varies with λ^{-4} it is much weaker at 438 than at 205 nm. Hence scattering off dust particles becomes important at 438 nm, which impedes the measurement of the vertical laser intensity profile by Rayleigh scattering. Therefore after every experiment the off resonant fluorescence in a very fuel-rich flame ($S_{ac} \geqslant 25\%$) is recorded, which is proportional to the laser power. The C_2 fluorescence image is then divided by the vertical laser intensity profile to obtain the laser power normalized C_2 fluorescence distribution. Absorption of the laser beam is found to be negligible.

When the natural emission of the flame is observed through the $\lambda \geqslant 470$ nm long-pass filter, only C_2 chemiluminescence is detected,[4] which is used to determine the dimensions of the acetylene feather and the flame front, as discussed above.

III. RESULTS AND DISCUSSION

A. Distribution of atomic hydrogen in the gas phase

The dependence of the H fluorescence signal on the laser power is shown in Fig. 1. From the quadratic fit to the data points it is clear that within the indicated error bars the LIF signal varies as the square of the laser power, implying that multi-photon ionization and/or laser induced photochemical processes producing atomic hydrogen do not occur or are negligible for the range of laser powers used in the experiments described in this work. The method of correction for the vertical power inhomogeneity in the laser sheet, as discussed above, is therefore valid.

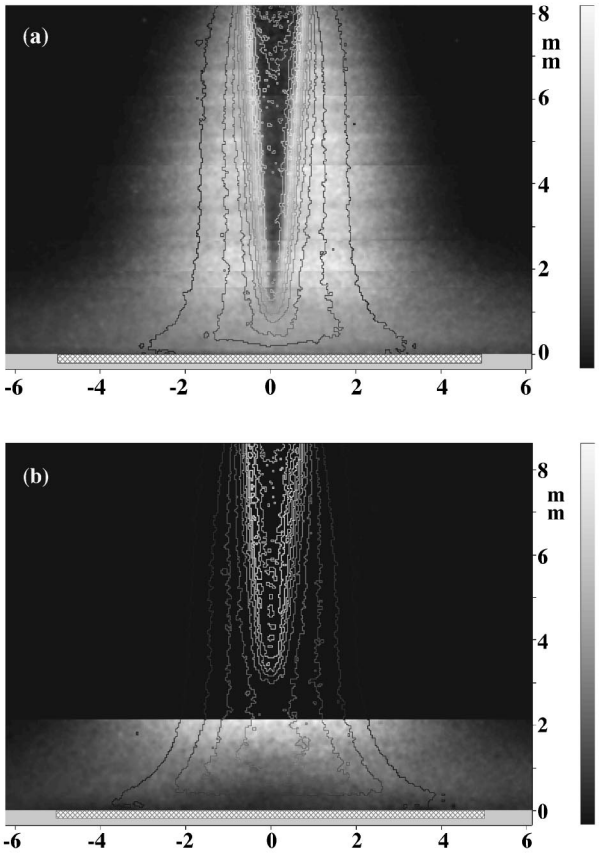

FIG. 2. H LIF signal (linear gray scale in arbitrary units, ranging from black (zero) to white (maximum)) during diamond deposition in the laminar flame, with the corresponding C_2 chemiluminescence superimposed (isophotes, representing equal intensity difference steps). (a) Flame-substrate distance d=0.85 mm; the image is constructed from six separate images recorded at different heights of the laser beam in the flame, each corrected for the vertical laser intensity distribution. The slight vertical inhomogeneity in the LIF signal between 1.6 and 8.2 mm above the substrate is due to the image construction. (b) Single image, corrected for the vertical intensity distribution of the laser beam (the noisy uppermost part is removed for reasons of clarity), d=3.05 mm. The laser beam travels from right to left through the flame, the substrate is indicated in gray and the burner tip is located just above the top of the image; the crosshatched area depicts the diamond deposition region, dimensions are in mm.

Figure 2 shows the spatial distribution of the laser power normalized atomic hydrogen fluorescence during diamond growth for two different flame - substrate distances d. The signal intensities (arbitrary units) are represented by gray values on a linear scale, ranging from black (zero intensity) to white (maximum intensity). In order to facilitate the interpretation of the images, in terms of flame structure, and the comparison to other measurements on flame deposition of diamond, the C_2 chemiluminescence as detected through the 656 nm interference filter is superimposed as isophotes on the H LIF distribution. The isophotes depict ten steps of equal intensity difference on a linear gray scale. In Fig. 2a the distribution of H fluorescence in nearly the whole cross section of the flame is shown for d=0.85 mm. This image is constructed from six separate images obtained at different

heights of the laser beam above the substrate. Due to artifacts in the image construction, some slight vertical inhomogeneities (''horizontal ripples'') are still visible between 1.6 and 8.2 mm above the substrate, but the large scale distribution of atomic hydrogen in the flame is clearly seen from this image. H is created at the flame front and diffuses rapidly throughout the flame, where it may be consumed and (re-)created by reactions with other species present. Comparison of the distribution of H to those of CH, C_2, CN, and OH, obtained in previous studies[4,48] and discussed below, shows that the radial distribution of hydrogen is nearly homogeneous inside the acetylene feather (which has a radius of ≈ 2 mm under the present flame operating conditions), except for the region below the tip of the flame front. Outside the acetylene feather the hydrogen signal decreases gradually, until H is consumed by reactions with ambient air to form OH, among other species. Below the tip of the flame front the distribution of atomic hydrogen is strongly influenced by the substrate and the diamond growth process taking place on it. Image construction artifacts are completely avoided in all other atomic hydrogen images, including the lower part of Fig. 2a (between 0 and 1.6 mm above the substrate). An example of the H LIF distribution at the relatively large flame-substrate distance of d=3.05 mm is shown in Fig. 2b. In this image the lower edge of the laser beam is below the substrate surface and the noisy upper edge of the H LIF signal (resulting from the division by the square of low laser intensities) is removed for reasons of clarity. Upon close inspection a minimum in H signal intensity is found above the center of the growing diamond layer at this value of d, in contrast to Fig. 2a, which is taken at a much smaller distance.

In general a dark boundary layer is observed just above the substrate under all deposition conditions, where the signal intensity is markedly lower than at larger distances above the substrate. In order to study the distribution of atomic hydrogen close to the substrate in more detail, horizontal and vertical profiles of the H LIF distribution are obtained for various growth conditions. Vertical profiles are given in Fig. 3; they show that for small d (0.85 mm) the H signal is non-zero close to the substrate and grows fast until 0.4 mm above the substrate, after which it is constant up to the flame front. This is in agreement with calculations of Matsui *et al.*,[19] Goodwin,[22] and Okkerse *et al.*[25] If the collisional quenching of fluorescence in a first approximation is assumed to be proportional to the pressure, its effect on the LIF signal can be estimated. Since pressure is proportional to temperature via the ideal gas law, the quenching would be proportional to the temperature, whence the LIF signal would be relatively higher in colder areas of the flame. Lacking experimental data on the temperature gradient, it can be taken from recent calculations by Okkerse, which show a rapid increase in the first ≈ 0.3 mm above the substrate, after which the temperature is nearly constant up to the flame front.[55] If the vertical H profile for d=0.85 mm is corrected for this, it follows the calculated profile more closely between 0.0 and 0.3 mm above the substrate. For distances d between flame front and substrate larger than 2 mm, the observed increase in H signal (Fig. 3) is much slower, and the gradient decreases with increasing d. The latter may be explained by the larger separation from the flame front, where atomic hydrogen is created. Recent calculations by Okkerse reveal that the gradient in the first 0.3 mm above the substrate is independent of d and that a maximum H concentration is reached at ≈ 0.6 mm above the substrate, for values of d up to 2.0 mm.[55]

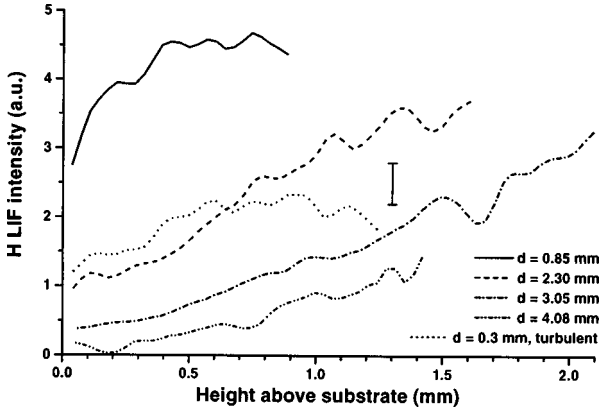

FIG. 3. Vertical profiles of the H LIF signal at the symmetry axis of the flame (laminar, except for d=0.3 mm). The distance d between substrate and flame front is given for each profile, together with a representative error bar (the local minimum in the d=3.05 mm profile between 1.50 and 1.75 mm above the substrate is due to an artifact).

For the turbulent flame the value of d=0.3 mm is determined from the averaged position of the flame front; the actual distance, however, between parts of the turbulent flame front and the substrate varies rapidly (movement can already be seen after 100 ns) between $\leqslant 0.1$ and $\geqslant 2.0$ mm. The H LIF signal, which is present below the actual turbulent flame front, can consequently also be observed at distances above 0.3 mm from the substrate. Another implication of the turbulence is that pockets of unburnt acetylene and oxygen are present close to the substrate, diminishing the averaged H LIF signal below 0.3 mm from the substrate and resulting in a much less steep gradient in the vertical profile close to the substrate than found in the laminar flame for d=0.85 mm.

The vertical gradient in the H LIF distribution close to the substrate is, apart from the flow geometry, due to reactions of atomic hydrogen in the gas phase with the growing diamond layer. It can stick to the surface or it can abstract adsorbed species like H, C, or CH_x from the surface to form H_2, CH, or CH_{x+1}, respectively, in the gas phase. The diamond surface hence acts as a sink for gas phase atomic hydrogen in its close proximity.

More information is obtained from the horizontal profiles of the H LIF distribution, which are shown in Fig. 4. Each profile is taken at 0.10 mm above the substrate. The lateral distribution of H shows a marked dependence on d: if the flame is close to the substrate (d=0.85 mm, Fig. 4a, compare to Fig. 2a) a maximum is found in the center and the signal decreases linearly with radial distance. At moderate distances the H distribution is uniform in the central area with a radius of 4–6 mm (Figs. 4b and 4c, respectively) and for larger distances (Figs. 4d and 4e, compare to Fig. 2b) a central minimum is developed. Although the turbulent flame is very close (d=0.3 mm) to the substrate, a central maxi-

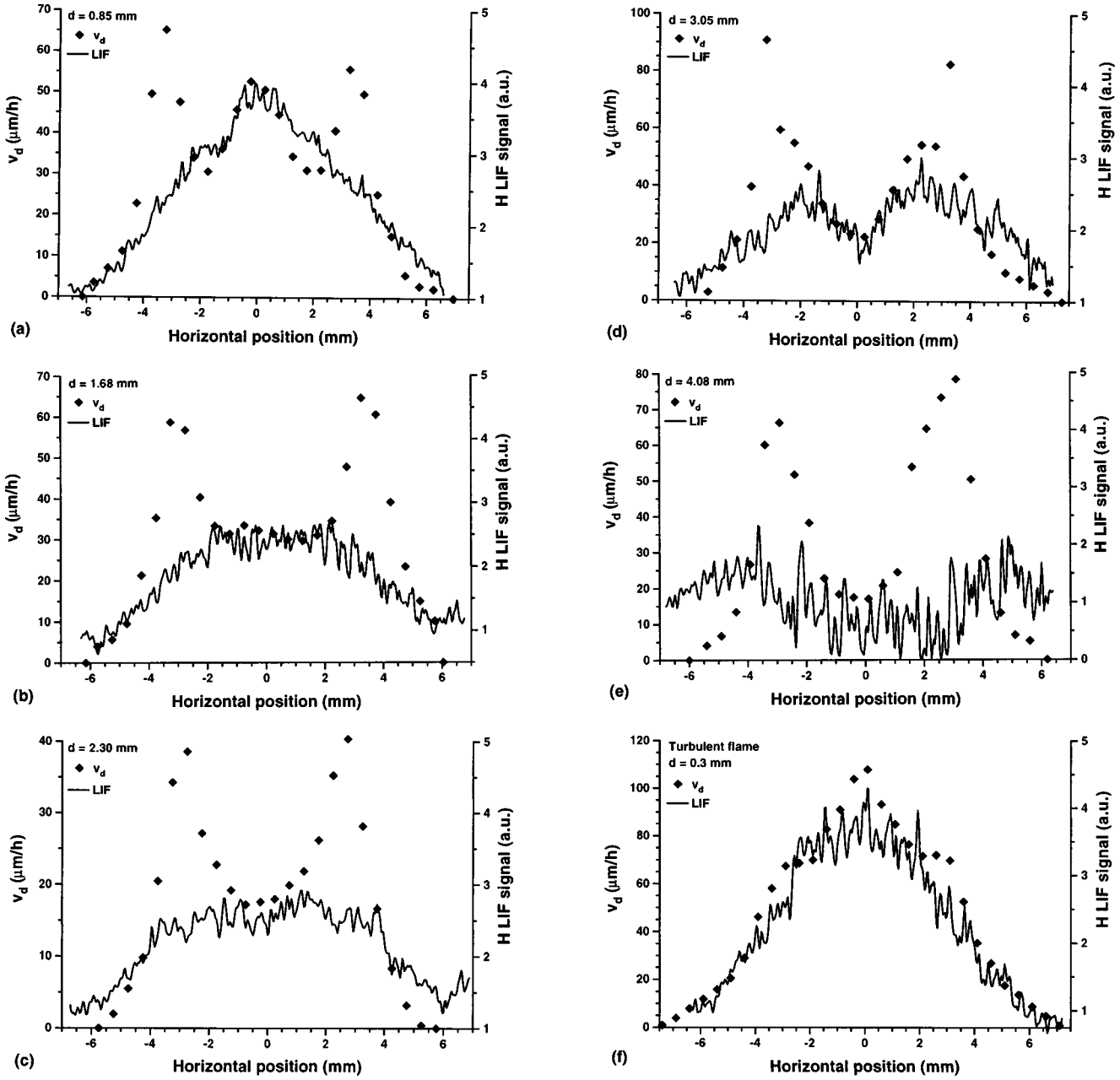

FIG. 4. Horizontal profiles of the H LIF signal at 0.10 mm above the substrate during diamond growth and the deposition rate v_d of the corresponding diamond layer along the path of the laser beam, for the laminar flame (a–e) and the turbulent flame (f). The distance d between flame front and substrate is indicated.

mum is not observed in the horizontal distribution of H in this flame. This is caused by the higher mixing rates in the turbulent flame compared to the laminar flame, which makes the species distribution in the central area of the flame more homogeneous.

Two additional diamond growth experiments have been carried out at deposition temperatures T_d different from the 1050 ± 20 °C used in the experiments described above, in order to determine whether T_d has an influence on the distribution of the H LIF signal in the flame. Although T_d is known to have a significant effect on the deposition rate, quality and morphology of flame grown diamond layers, as observed by Schermer and co-workers,[49] no difference in the spatial distribution of the H LIF signal could be detected above noise level in the two additional experiments, in which $T_d = 950$ and 1150 °C has been used, respectively. Also, in the previous study on C_2 and CH during diamond growth,[4] no influence of T_d on the gas phase distribution of those molecules has been found. This suggests that T_d is not very important for gas phase processes involving these species.

B. Distribution of C_2 in the gas phase

The two-dimensional distribution of C_2 at relatively small distances d between flame front and substrate (less than 2 mm) has been described elaborately in the previous work on C_2.[4] Figure 5a shows the presence of C_2 at the larger distance of 2.80 mm. The highest C_2 LIF signal is

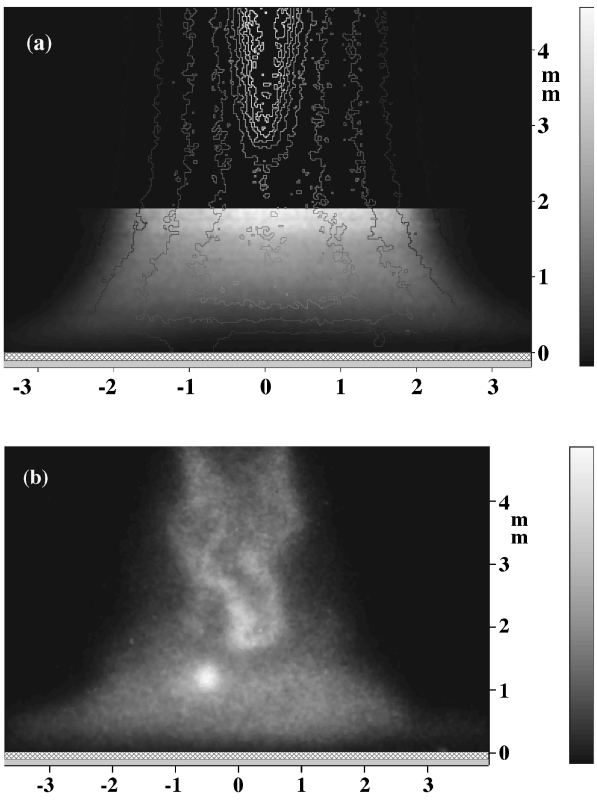

FIG. 5. (a) C_2 LIF signal (linear gray scale in arbitrary units, ranging from black (zero) to white (maximum)) during diamond deposition in a laminar flame at d=2.80 mm, with the corresponding C_2 chemiluminescence superimposed (isophotes, representing equal intensity difference steps). The image is corrected for the vertical intensity distribution of the laser beam (the noisy uppermost part is removed for reasons of clarity). (b) Single 10 ns snapshot of the turbulent flame (average distance d=0.49 mm), revealing C_2 chemiluminescence combined with C_2 LIF signal. The laser sheet reaches to 2.5 mm above the substrate. The laser beam travels from right to left through the flames, the substrate is indicated in gray and the burner tip is located above the top of the image; the outer edges of the diamond deposition region are not shown, dimensions are in mm.

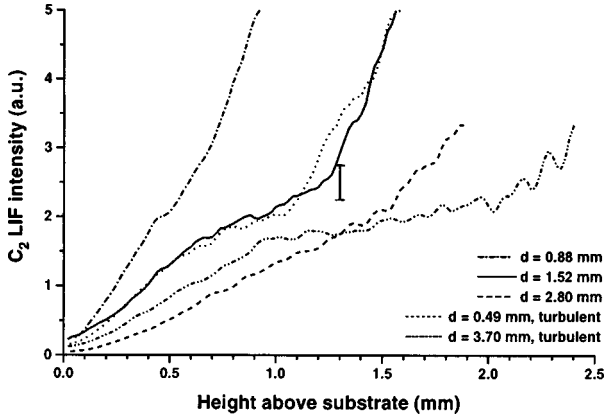

FIG. 6. Vertical profiles of the C_2 LIF signal at the symmetry axis of the laminar and turbulent flames. The distance d between substrate and flame front is given for each profile, together with a representative error bar. The three profiles for d=0.49, 0.88, and 1.52 are normalized to have the same maximum intensity, because the flame front is located within the laser sheet.

expected at the flame front, which is, however, above the upper edge of the laser sheet. The dark boundary layer can be clearly seen above the substrate, and in the central 2 mm it is thicker than further outside. The distribution of C_2 is limited to the flame front and the entire acetylene feather, as already discussed in Ref. 4.

The capricious character of the flame on the turbulent burner can be seen in Fig. 5b, which shows a single 10 ns snapshot of the turbulent flame with the laser tuned to the resonance, freezing the motion of the flame front. The background of C_2 chemiluminescence is still visible and shows that the outer edge of the acetylene feather is much less turbulent than the flame front itself. The laser sheet reaches to 2.5 mm above the substrate and the C_2 LIF signal is superimposed onto the C_2 chemiluminescence between the tip of the flame front and the substrate. In Fig. 5b the boundary layer is also clearly visible.

The increase of the C_2 LIF signal from the substrate towards the tip of the flame front is given in Fig. 6. It is clear that the C_2 signal in the laminar flame increases nearly uniformly for d=0.88 and 2.80 mm, but for d=1.52 mm a sudden change in the gradient is observed at 1.25 mm above the substrate. This sudden change of gradient may also be present for d=2.80 mm, but then it may be located above the upper edge of the laser sheet and therefore not be visible in Fig. 6. The nearly uniform increase of C_2 for d=0.88 mm is similar to theoretical predictions by Okkerse *et al.*[25] Recent calculations by Okkerse for larger values of d reveal that a gradual increase of C_2 may also be expected in the first 1.0–1.5 mm above the substrate for d=1.52 and 2.80 mm and that the gradient decreases with increasing d.[55] In the turbulent flame the C_2 signal increases as well up to and beyond the averaged position of the flame front, and for d=3.70 mm the C_2 gradient suddenly changes at 0.9 mm above the substrate.

The behavior of C_2 on the flame axis (Fig. 6) can be compared to that of H (Fig. 3) for a few experiments where the values of d are not far apart. For d=0.85/0.88 mm it is remarkable that C_2 steadily increases up to the flame front, whereas H reaches a constant level already at 0.4 mm above the substrate. In the turbulent flame close to the substrate (d=0.30/0.49 mm) the H signal is more or less constant in the whole measurement volume, but the C_2 signal grows up to 1.0 mm above the substrate and above that height increases even faster. At the relatively large distance of d=2.80/3.05 mm, however, both H and C_2 steadily increase with the height above the substrate. The differences in H and C_2 behavior for small to moderate values of d can possibly be ascribed to the larger diffusion coefficient for atomic hydrogen (with respect to that of the much heavier C_2 molecule), and the fact that atomic hydrogen, in contrast to C_2, often needs a third body in chemical reactions, which may reduce its reaction rate compared to that of C_2.

Horizontal profiles of the C_2 LIF distribution are obtained at 0.10 mm above the substrate and are shown in Fig. 7. The trend in the central 4 mm of the profiles is similar to that observed for atomic hydrogen in the same region: at small distances d a clear central maximum is found, which changes into a uniform distribution at moderate distances and into a central minimum at relatively large d. The presence of C_2 is, in contrast to atomic hydrogen, limited to the

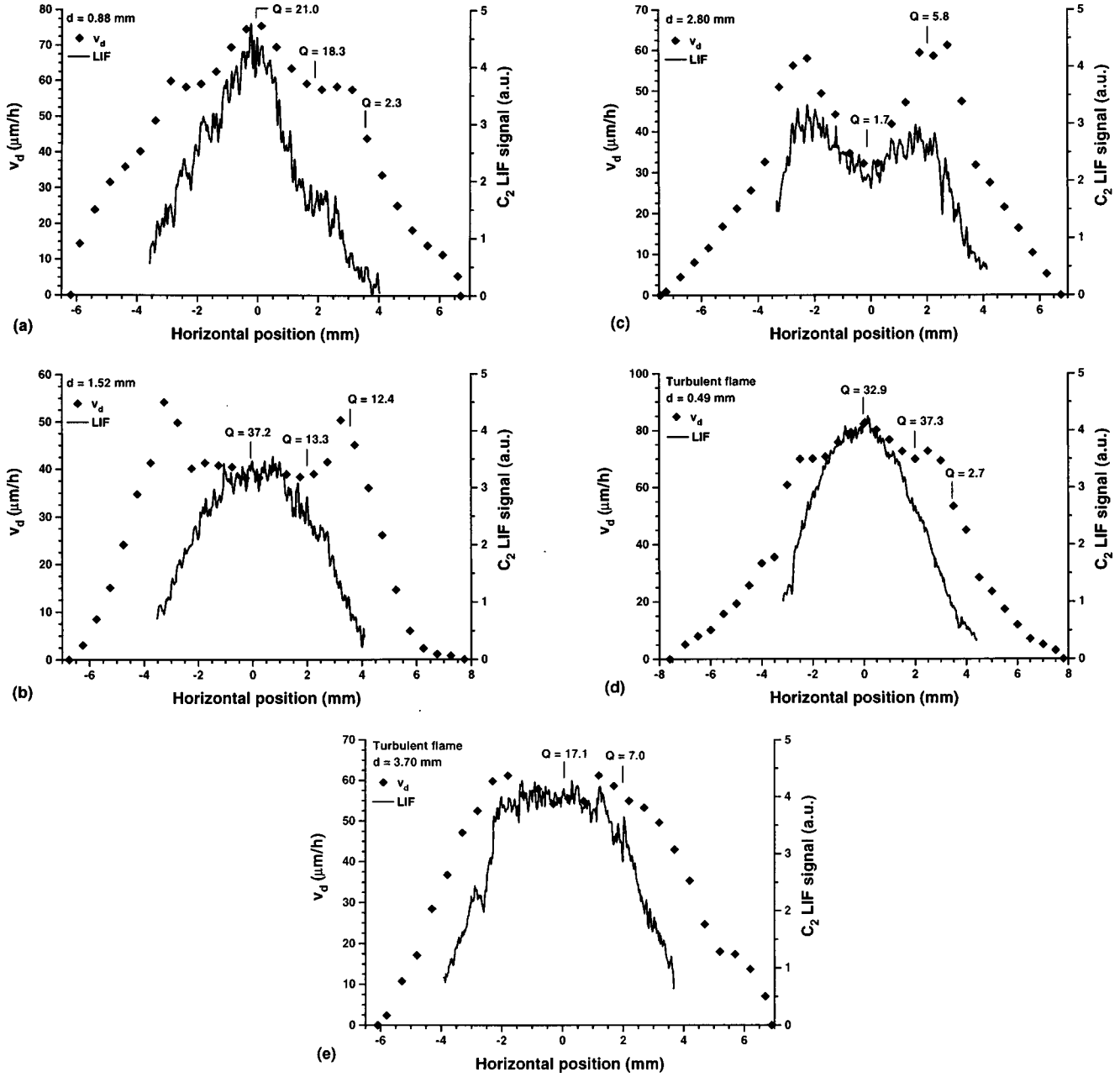

FIG. 7. Horizontal profiles of the C_2 LIF signal at 0.10 mm above the substrate during diamond growth and the deposition rate v_d of the corresponding diamond layer along the path of the laser beam, for the laminar flame (a–c) and the turbulent flame (d–e). Q is the quality of the diamond layer at different radial positions, as determined from Raman spectra. The distance d between flame front and substrate is indicated.

acetylene feather, which is why the C_2 signal falls off much more rapidly at larger radial distances than the H signal. The characteristic distributions of H and C_2 close to the substrate will be determined not only by the chemistry taking place, but also by the flow geometry of the flame gases impinging on the substrate.

C. Diamond growth

1. Morphology and growth rate

The morphology of the deposited diamond layers obtained in this study is similar to that described in previous work, where SEM photographs are given,[4,48] and in work of Schermer *et al.*[49–51,56] Specimens grown relatively close to the flame front have a continuous central area of well connected randomly oriented crystallites with {111} and {100} facets. Samples grown at larger distances in the laminar flame ($d>2.5$ mm), however, reveal a less homogeneous central area and show an additional core zone in the middle of this region, where the crystallites are much smaller than found at lower d values.[48,50] Outside the central region a so-called annulus of enhanced growth is observed (as discussed below), which exhibits large columnar crystallites separated by voids or embedded in an amorphous layer of cauliflower-like features. These crystallites frequently have {100} top facets almost parallel to the substrate, but the side facets are curved, highly twinned and reveal amorphous features. Beyond this annulus of enhanced growth and roughness the deposits have the same structure as the central re-

gion, but the size of the crystallites decreases with increasing radial distance from the center. The specimen grown by the turbulent flame at d=0.30 mm is deposited so close to the flame front that the central region of 2 mm diameter does not form a continuous layer anymore, but is broken up into separate crystallites revealing a relatively high growth rate.

The local variation of the deposition rate v_d along the path of the laser beam is given together with the radial H or C_2 LIF signal distribution in the boundary layer in Figs. 4 and 7, respectively. The distance d between the substrate and the flame front turns out to have a large influence on the growth rate of the central region of 4–5 mm diameter of the diamond layer. For d between 0.8 and 0.9 mm (Figs. 4a and 7a) a large central maximum is observed with v_d between 55 and 75 μm/h, which changes into a central area of uniform growth rate (30–40 μm/h) around d=1.5 - 1.6 mm (Figs. 4b and 7b). At larger distances d this is replaced by a shallow to deep central minimum (Figs. 4c, d, e, and 7c, respectively) with the growth rate decreasing correspondingly to only 17 μm/h at d=4.08 mm. The diamond layers deposited by the turbulent flame at small distances d have a central maximum as well (Figs. 4f and 7d), but at d=3.70 mm (Fig. 7e) the central region still has a uniform growth rate, due to the better mixing of flame gases in the turbulent flame, as opposed to the laminar flame.

The annulus of enhanced growth, with a radius of 3.0–3.5 mm, is found outside the central region. Its deposition rate shows a pronounced local maximum which, excepting small values of d, is higher than the growth rate of the central region and changes much less significantly with d, as can be seen in Figs. 4 and 7. The dependence of the radial variation of v_d on the distance d agrees well with findings from previous experiments in the same setup.[4,48] The growth rate of the center of the diamond layers agrees well with results obtained in the similar setup of Schermer and co-workers.[49,50] Small differences in the absolute value of v_d as well as in its local variation, as observed between diamond layers deposited under nearly equal growth conditions, may be due to a slightly different gas composition in the acetylene and oxygen bottles. The importance of the exact gas bottle contents, including minor contaminations, has been described previously,[48] and may even play a role if two acetylene bottles from the same supplier are concerned, which is the case in Figs. 4a and 7a, respectively.

2. Relation with atomic hydrogen

When the variation of v_d is compared to the radial distribution of H LIF signal in the boundary layer, it is striking that both show a very similar radial behavior from the center all the way to the edge of the diamond layer, if the annulus of enhanced growth is not taken into account. This is true for the laminar flame (Figs. 4a–4e) as well as the turbulent flame (Fig. 4f), although for the latter the correspondence in the central 2 mm is not as good, which may be due to the very small distance between the substrate and the actual flame front, as discussed before. The anomalous behavior of v_d in the annulus of enhanced growth can be ascribed to the influence of ambient air diffusing into and reacting with the flame, creating CN and related species which have an additional positive effect on the local growth rate (as discussed in a previous study[48] and references therein). The good agreement between the H distribution in the boundary layer and v_d (apart from the annulus of enhanced growth) indicates the importance of atomic hydrogen to the deposition rate of the diamond layer, which has already been studied elaborately in theory.[12,15–17,21,24,26] At the edge of the diamond layer atomic hydrogen is still found in measurable quantities, but diamond growth here is limited by the lack of carbon containing species. Further outside H reacts with ambient O_2 to form OH, as described above.

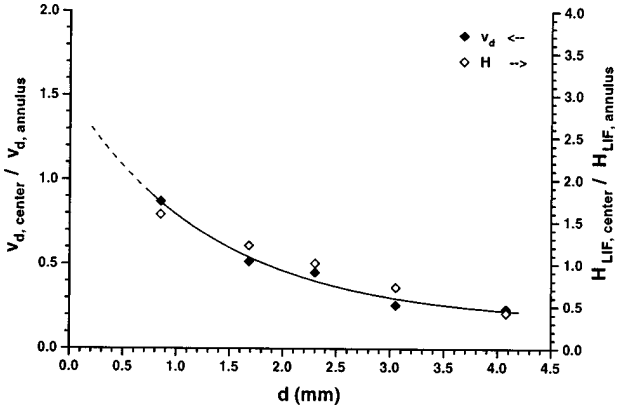

FIG. 8. Ratios of the deposition rate v_d (solid symbols, left-hand ordinate) and of the H LIF signal (open symbols, right-hand ordinate) as observed in/above the center and the annulus of enhanced growth of the diamond layers, vs distance d between flame front and substrate (data obtained from Fig. 4). The solid line is an exponential fit to $v_{d,\mathrm{center}}/v_{d,\mathrm{annulus}}$, which is extrapolated to smaller d values.

Although the H LIF signal is measured in arbitrary units and therefore cannot be compared on an absolute scale from one experiment to another, it is meaningful to compare the (dimensionless) ratios of the signal at different positions within a single growth experiment. In Fig. 8 the ratio of the H LIF signal above the center ($H_{\mathrm{LIF,center}}$) and above the annulus of enhanced growth ($H_{\mathrm{LIF,annulus}}$) of the diamond layer, as obtained from Fig. 4, is plotted versus d, together with the ratio of v_d in the central region ($v_{d,\mathrm{center}}$) and in the annulus of enhanced growth ($v_{d,\mathrm{annulus}}$). With $v_{d,\mathrm{annulus}}$ being roughly constant, as mentioned above, the decrease of $v_{d,\mathrm{center}}$ with d agrees with results obtained in other diamond flame deposition experiments[4,48–50] and an exponential fit can be made, as argued by Schermer and co-workers.[50]

In the laminar flame the ratio $H_{\mathrm{LIF,center}}/H_{\mathrm{LIF,annulus}}$ follows nearly the same exponential decay as $v_{d,\mathrm{center}}/v_{d,\mathrm{annulus}}$. From Fig. 8 it is also clear that $H_{\mathrm{LIF,center}}/H_{\mathrm{LIF,annulus}} \approx 2 \times v_{d,\mathrm{center}}/v_{d,\mathrm{annulus}}$ in the laminar flame. If the diamond deposition rate is assumed to be directly proportional to the distribution of atomic hydrogen over the entire diamond layer (not considering for the sake of argument other vital factors such as the presence of carbon containing species), this would mean that $v_{d,\mathrm{annulus}}$ is about twice as large as might be expected from the H distribution. Hence $v_{d,\mathrm{annulus}}$ could then be thought of as the result of two equally important processes: one being ''normal'' diamond growth, due to species originating from the combustion of acetylene with oxygen, the other one ''additional'' diamond growth, caused

by species created in the reactions of ambient air with flame gases. In the turbulent flame it is much more difficult to make this distinction, for there the flame species are better mixed.

3. Relation with C_2

From a previous study it is already known that in the central area of the laminar flame the distribution of C_2 in the boundary layer resembles the variation of v_d up to d=1.4 mm.[4] At small d values a maximum in the C_2 distribution is observed, which turns into a minimum at large d values. The atomic hydrogen distribution and v_d reveal the same behavior. From Fig. 7 it follows that the similarity extends to larger d values and to the turbulent flame as well. Above the annulus of enhanced growth, however, the C_2 signal has already dropped significantly. The resemblance indicates that C_2 may be important for the diamond growth rate in the center of the deposited layer, which agrees with the role of C_2 as a diamond precursor, as put forward by Gruen and co-workers.[43–47] An explanation for the anomalous behavior of the annulus of enhanced growth has been given above and in Ref. 48. Further outside the annulus the C_2 signal diminishes rapidly, since its presence is limited to the acetylene feather. At the edge of the feather C_2 reacts with ambient O_2 and OH[57] and diamond growth outside the annulus may be due to H and CN or related species (as discussed before and in Ref. 48). In contrast to atomic hydrogen, no clear relation between the ratio $C_{2,\mathrm{center}}/C_{2,\mathrm{annulus}}$ of the LIF signal and $v_{d,\mathrm{center}}/v_{d,\mathrm{annulus}}$ is observed.

The quality Q of the diamond layers is obtained from Raman spectra, taken along the path of the laser sheet at radially different positions within the deposits. Figure 7 shows the values of Q together with v_d and the distribution of C_2 LIF at 0.10 mm above the corresponding diamond layer. As has been discussed in the previous study on C_2 during diamond growth,[4] a relation is observed in Fig. 7 between the radial variation of Q and the flame-substrate distance d. Comparison of Figs. 4 and 7 reveals that in the laminar flame at a small d value Q as well as the LIF signals of H and C_2 show a maximum in the center, and all three decrease when moving radially away from the center. For relatively large d, Q is lower in the center than 2 mm outside it, similar to the H and C_2 distributions. In the turbulent flame Q first slightly increases towards the annulus of enhanced growth at d=0.49 (Fig. 7d), but at d=3.70 mm the trend resembles that in the deposits of the laminar flame. In the experiment performed at d=2.80 mm (Fig. 7c) S_{ac}=8% has been used instead of S_{ac}=5%, as applied in all the other experiments described here. This results in lower Q values for the whole diamond layer,[49] but the radial variation of Q within this layer is still clearly visible. Considering the dependence on d of the distributions of H and C_2 just above the diamond layer and the radial variation of Q within the deposited layer, it is suggested a relation between Q and the H distribution exists. Unfortunately, there was no possibility to measure Raman spectra and determine Q values for the specimens for which the H distribution was measured. As far as C_2 is concerned, a similar relation may exist with Q, which would then be limited to the center of the diamond layer.

IV. CONCLUSIONS

The diamond growth process in both laminar and turbulent flames has been studied in detail and the distributions of atomic hydrogen and C_2 have been visualized using the two-dimensional laser induced fluorescence technique. If high UV laser powers are avoided, a few 205 nm laser shots are in principle sufficient to detect a two-photon LIF signal of H in the plane of the laser sheet. Once the quadratic power dependence of the H LIF signal is established, the images can be corrected for inhomogeneities in the laser beam and the atomic hydrogen distribution in the flame can be determined in an area of more than 12×2 mm^2. Atomic hydrogen is omnipresent at and beyond the flame front to well outside the acetylene feather, where it is finally consumed by reactions with ambient air. During deposition the gas phase boundary layer above the entire growing diamond layer is filled with H. For small flame-substrate distances (d$<$1 mm) a central maximum is found which changes into a uniform distribution at larger distances. Under the present deposition conditions a shallow to deep central minimum develops above the diamond deposit for d$>$2.3 mm.

A strong relation is observed between the distribution of H in the gas phase boundary layer just above the diamond and the radial variation of the growth rate: the diamond growth rate matches the horizontal distribution of atomic hydrogen very well over the whole deposition area, except for the annulus of enhanced growth, in both laminar and turbulent flames. This relation is already expected from theoretical calculations on diamond growth.[12,15–17,21,24,26] The growth rate of the annulus of enhanced growth is about twice what can be expected from the H signal in the gas phase. This can be explained by the presence of CN and related species above the annulus, created by the diffusion of ambient air into the flame, which have an additional positive effect on the diamond growth rate, as has already been described in a previous study.[48]

The distribution of C_2 has been studied under comparable conditions, which are complementary to earlier work.[4] C_2 is found at the flame front and in the entire acetylene feather, the outer edge of which is also the limit of the C_2 presence. The horizontal distribution of C_2 in the boundary layer above the central region ($\approx$4 mm diameter, i.e., inside the annulus of enhanced growth) of the growing diamond layer resembles that of atomic hydrogen. A clear relation between C_2 in the gas phase and the growth rate of this central region has been observed, as described before.[4] This relation confirms the importance of C_2 as a possible diamond precursor for the central region of the layer, in accordance with theoretical as well as experimental results of Gruen *et al.*[43–47] In their results of diamond growth from C_{60} it was demonstrated that atomic hydrogen is not necessary for diamond growth, but in the oxyacetylene flame described here, both H and C_2 are expected to be important, although the importance of C_2 appears to be restricted to the center of the diamond layer. A possible relation is observed between the

radial variation of the quality of the diamond layer, as determined from Raman spectra, and the distributions of H and C_2 above the center and the annulus of enhanced growth of the deposited layer. This agrees with the previously found relation between the quality and the C_2 distribution.[4]

Vertical profiles of both the H and C_2 distribution on the symmetry axis of the flame have been determined. Close to the substrate the C_2 signal approaches zero, but the H signal appears to remain non-zero under all deposition conditions. For both species the gradient is smaller if the flame is located at a larger distance from the substrate. The profiles obtained for H and C_2 with the laminar flame at about 0.9 mm above the substrate agree with calculations of Okkerse *et al.*[25]

The aforementioned relations between C_2 and H and the diamond growth rate, combined with the distribution of OH and CN during diamond deposition[4,48] and the observed morphology of the deposited diamond layers,[4,48–51,56] suggest that three separate regions can be distinguished in the gas phase above the diamond layer. The first region is the center of the flame, beyond the flame front, where all species present are created by the combustion of acetylene (C_2H_2) with oxygen (including possible source gas contaminations). These species include C_2, CH, H, H_2, and possibly CH_3. Above the growing diamond layer this central region extends to, but does not include, the annulus of enhanced growth. Properties like growth rate, morphology, and impurity incorporation of the center of the diamond layer, which reveals a continuous layer of well connected randomly oriented crystallites with {111} and {100} facets, are solely and completely determined, as far as the gas phase is concerned, by the exact gas composition of this central region. The second region is the outer edge of the acetylene feather, where the influence of ambient air diffusing into the flame is noticed by the creation of nitrogen containing species like CN and possibly NH and the rapid decrease of species like C_2 and CH created from the flame source gases. Close to the substrate this region is limited to the annulus of enhanced growth, whose characteristics are determined by both the ambient atmosphere and the flame source gases. Atomic hydrogen is still present in considerable quantities in this region. The annulus of enhanced growth exhibits large columnar crystallites, frequently with {100} top facets almost parallel to the substrate, separated by voids or embedded in an amorphous layer of cauliflower-like features. The third region surrounds the acetylene feather and contains species like OH, H_2O, CO, CO_2, and, close to the acetylene feather, still some CN. Atomic hydrogen is consumed by reactions with ambient species. Diamond growth in this region is limited by the rapid decrease of carbon containing species and atomic hydrogen, and the diamond layer properties are somewhat less dependent on the flame source gas composition than in the center and the annulus of enhanced growth. The morphology in this region resembles that of the central region, with the size of the crystallites diminishing fast at increasing radial distance.

Under the deposition conditions used in the present work, all three regions are of interest to diamond growth. If the flame-substrate distance is increased, the intersection of the central region in the gas phase with the substrate becomes smaller and the center of the diamond layer starts deteriorating, the first indication of which is the appearance of the core zone[48,50] if the flame front is more than 2.5 mm above the substrate. At larger distances the central region in the gas phase eventually no longer touches the substrate and diamond growth only occurs in the annular second region, which has also been found by Cappelli and Paul[58] and Abe *et al.*[59,60] in different experimental setups. It is therefore important for the purpose of comparing the results of different experimental setups to specify the distance d between the flame front and the substrate, and not only the burner-to-substrate distance, together with the total gas flows and burner orifice diameter.

The observed relations between H and C_2 and the properties of the obtained diamond layers not only elucidate the growth process, but also show that both signals are important indicators in the flame growth of diamond. If monitored during growth, they can be used to adjust the process to obtain diamond layers with properties closer to those desired for (industrial) applications.

ACKNOWLEDGMENTS

The authors wish to thank Ir. J. J. Schermer for performing the Raman measurements and, together with Ir. M. Okkerse and Dr. W. J. P. van Enckevort, for many useful discussions. This work has been made possible by the financial support of the Stichting voor Technische Wetenschappen (Technology Foundation).

[1] *The Properties of Diamond*, edited by J. E. Field (Academic, London, 1979).
[2] K. E. Spear and J. P. Dismukes, *Synthetic Diamond, Emerging CVD Science and Technology* (Wiley, New York, 1994).
[3] Y. Hirose and N. Kondo, Extended Abstracts, 35th Japanese Applied Physics Spring Meeting, March 1988 (unpublished), p. 434.
[4] R. J. H. Klein-Douwel, J. J. L. Spaanjaars, and J. J. ter Meulen, J. Appl. Phys. **78**, 2086 (1995).
[5] K. E. Spear, J. Am. Ceram. Soc. **72**, 171 (1989).
[6] J. C. Angus, H. A. Will, and W. S. Stanko, J. Appl. Phys. **39**, 2915 (1968).
[7] F. G. Celii and J. E. Butler, Annu. Rev. Phys. Chem. **42**, 643 (1991).
[8] J. E. Butler and R. L. Woodin, Philos. Trans. R. Soc. London, Ser. A **342**, 209 (1993).
[9] M. Page and D. W. Brenner, J. Am. Chem. Soc. **113**, 3270 (1991).
[10] D. Huang and M. Frenklach, J. Phys. Chem. **96**, 1868 (1992).
[11] B. B. Pate, M. H. Hecht, C. Binns, I. Lindau, and W. E. Spicer, J. Vac. Sci. Technol. **21**, 364 (1982).
[12] G. Janssen, W. J. P. van Enckevort, and L. J. Giling, in *Proceedings of the First International Symposium on Diamond and Diamond-like Films*, edited by J. P. Dismukes (Electrochemical Society, Pennington, NJ, 1989), p. 508.
[13] T. R. Anthony, Vacuum **41**, 1356 (1990).
[14] W. A. Yarbrough and R. Messier, Science **247**, 688 (1990).
[15] M. Frenklach and K. E. Spear, J. Mater. Res. **3**, 133 (1988).
[16] M. Frenklach, J. Appl. Phys. **65**, 5142 (1989).
[17] M. Frenklach and H. Wang, Phys. Rev. B **43**, 1520 (1991).
[18] Y. Matsui, A. Yuuki, M. Sahara, and Y. Hirose, Jpn. J. Appl. Phys., Part 1 **28**, 1718 (1989).
[19] Y. Matsui, H. Yabe, and Y. Hirose, Jpn. J. Appl. Phys., Part 1 **29**, 1552 (1990).
[20] S. J. Harris, Appl. Phys. Lett. **56**, 2298 (1990).
[21] S. J. Harris and D. G. Goodwin, J. Phys. Chem. **97**, 23 (1993).
[22] D. G. Goodwin, Appl. Phys. Lett. **59**, 277 (1991).
[23] D. G. Goodwin, J. Appl. Phys. **74**, 6888 (1993).
[24] D. G. Goodwin, J. Appl. Phys. **74**, 6895 (1993).
[25] M. Okkerse, R. J. H. Klein-Douwel, M. H. J. M. de Croon, C. R. Kleijn, J. J. ter Meulen, G. B. Marin, and H. E. A. van den Akker, in *Chemical*

Vapour Deposition Proceedings of the Fourteenth International Conference and EUROCVD-11, edited by M. D. Allendorf and C. Bernard (Electrochemical Society, 1997), p. 163.
[26] A. Ohl, J. Röpcke, and C. Schleinitz, Diamond Relat. Mater. **2**, 298 (1993).
[27] J. E. Butler, B. D. Thoms, M. McGonigal, J. N. Russell, Jr., and P. E. Pehrsson, in *Wide Band Gap Electronic Materials*, edited by M. A. Prelas *et al.* (Kluwer, Dordrecht, 1995), p. 105.
[28] F. G. Celii and J. E. Butler, Appl. Phys. Lett. **54**, 1031 (1989).
[29] U. Meier, K. Kohse-Höinghaus, L. Schäfer, and C.-P. Klages, Appl. Opt. **29**, 4993 (1990).
[30] M. Chenevier, J. C. Cubertafon, A. Campargue, and J. P. Booth, Diamond Relat. Mater. **3**, 587 (1994).
[31] D. P. Dowling, T. P. O'Brien, E. M. Davitt, K. Donelly, T. C. Kelly, H. F. Doebele, V. Kornas, W. G. Graham, R. Cheshire, M. Higgins, and T. Morrow, Diamond Relat. Mater. **3**, 702 (1994).
[32] K. Donelly, D. P. Dowling, T. P. O'Brien, A. O'Leary, T. C. Kelly, R. Cheshire, K. F. Al-Assadi, W. G. Graham, T. Morrow, V. Kornas, V. Schulz-von der Gathen, and H. F. Döbele, Diamond Relat. Mater. **4**, 324 (1995).
[33] M. Chenevier, A. Gicquel, and J. C. Cubertafon, in Applications of Diamond Films and Related Materials: Third International Conference, 1995, edited by A. Feldman, Y. Tzeng, W. A. Yarbrough, M. Yoshikawa, and M. Murakawa (unpublished), p. 305.
[34] J. E. M. Goldsmith, Opt. Lett. **10**, 116 (1985).
[35] J. E. M. Goldsmith, Opt. Lett. **11**, 416 (1986).
[36] J. E. M. Goldsmith and R. J. M. Anderson, Appl. Opt. **24**, 607 (1985).
[37] U. Meier, K. Kohse-Höinghaus, and Th. Just, Chem. Phys. Lett. **126**, 567 (1986).
[38] J. E. M. Goldsmith, J. Opt. Soc. Am. B **6**, 1979 (1989).
[39] S. Agrup, F. Ossler, and M. Aldén, Appl. Phys. B: Lasers Opt. **61**, 479 (1995).
[40] J. Bittner, K. Kohse-Höinghaus, U. Meier, and Th. Just, Chem. Phys. Lett. **143**, 571 (1988).
[41] M. G. Allen, R. D. Howe, and R. K. Hanson, Opt. Lett. **11**, 126 (1986).
[42] C. Kaminski and P. Ewart, Appl. Phys. B: Lasers Opt. **61**, 585 (1995).
[43] D. M. Gruen, S. Liu, A. R. Krauss, and X. Pan, J. Appl. Phys. **75**, 1758 (1994).
[44] D. M. Gruen, S. Liu, A. R. Krauss, J. Luo, and X. Pan, Appl. Phys. Lett. **64**, 1502 (1994).
[45] D. M. Gruen, C. D. Zuiker, A. R. Krauss, and X. Pan, J. Vac. Sci. Technol. A **13**, 1628 (1995).
[46] D. A. Horner, L. A. Curtiss, and D. M. Gruen, Chem. Phys. Lett. **233**, 243 (1995).
[47] P. C. Redfern, D. A. Horner, L. A. Curtiss, and D. M. Gruen, J. Phys. Chem. **100**, 11654 (1996).
[48] R. J. H. Klein-Douwel, J. J. Schermer, and J. J. ter Meulen, Diamond Relat. Mater. (accepted for publication).
[49] J. J. Schermer, J. E. M. Hogenkamp, G. C. J. Otter, G. Janssen, W. J. P. van Enckevort, and L. J. Giling, Diamond Relat. Mater. **2**, 1149 (1993).
[50] J. J. Schermer, W. A. L. M. Elst, and L. J. Giling, Diamond Relat. Mater. **4**, 1113 (1995).
[51] J. J. Schermer and F. K. de Theije (work in progress).
[52] P. Alers, W. Hänni, and H. E. Hintermann, Diamond Relat. Mater. **2**, 393 (1993).
[53] J. J. Schermer, L. J. Giling, and P. Alers, J. Appl. Phys. **78**, 2376 (1995).
[54] R. W. B. Pearse and A. G. Gaydon, in *The Identification of Molecular Spectra* (Chapman and Hall, London, 1976), p. 83.
[55] M. Okkerse (private communication).
[56] G. Z. Cao, J. J. Schermer, W. J. P. van Enckevort, W. A. L. M. Elst, and L. J. Giling, J. Appl. Phys. **79**, 1357 (1996).
[57] A. G. Gaydon and H. G. Wolfhard, in *Flames, Their Structure, Radiation and Temperature* (Chapman and Hall, London, 1979), pp. 254, 255.
[58] M. A. Cappelli and P. H. Paul, J. Appl. Phys. **67**, 2596 (1990).
[59] T. Abe, M. Suemitsu, N. Miyamoto, and N. Sato, Appl. Phys. Lett. **59**, 911 (1991).
[60] T. Abe, M. Suemitsu, N. Miyamoto, and N. Sato, J. Appl. Phys. **73**, 971 (1993).